1979AN....300..151S

Astron. Nachr., Bd. 300, H. 3 (1979)

Force-free Magnetic Field Extrapolation for the Complex Sunspot Group of August 1972

N. SEEHAFER and J. STAUDE, Potsdam

Zentralinstitut für Solar-Terrestrische Physik der AdW der DDR

Sonnenobservatorium Einsteinturm

With 8 Figures (Received 1978 October 12)

Quantitative data on the magnetic field structure at all levels of the solar atmosphere are of basic importance for our understanding of physical processes in active regions in general and in flares in particular. Because photospheric longitudinal magnetograms are the most reliable data available, one has to look for a method of theoretical extrapolation of such data to higher levels. Such a method has been developed for force-free magnetic fields, i.e., $\nabla \times \boldsymbol{B} = \alpha \boldsymbol{B}$, with α = constant, satisfying more realistic boundary conditions as compared with earlier papers; e.g., the net magnetic flux through the magnetogram area is not required to be zero. The method has been used to calculate the magnetic field vector and lines of force in the flare-active region of August 1972. Calculated fields are compared with other observations such as structures in Hα. Results of August 3rd show that the loop prominence systems observed during the flares of August 2nd and 4th are represented by a force-free field with positive α rather than by a current-free field ($\alpha = 0$). The extractable energy supply of this force-free field is of the order of magnitude of maximum flare demand (10^{32} erg); the height dependence of the magnetic field strengths agrees with that from radio and X-ray estimates. Similar results are obtained for the August 7th magnetic field structure.

Für unser Verständnis der physikalischen Prozesse in aktiven Gebieten im allgemeinen und in Flares im besonderen ist es unbedingt erforderlich, quantitative Daten über die Magnetfeldstruktur in allen Niveaus der Sonnenatmosphäre zu erhalten. Da als zuverlässige Daten nur Longitudinal-Magnetogramme im Photosphärenniveau zur Verfügung stehen, muß man eine Methode entwickeln, um diese Daten nach höheren Niveaus hin zu extrapolieren. Für kraftfreie Magnetfelder, d. h. $\nabla \times \boldsymbol{B} = \alpha \boldsymbol{B}$, mit α = const. wurde eine solche Methode entwickelt, die im Vergleich zu früheren Arbeiten realistischere Randbedingungen erfüllt; z. B. wird nicht verlangt, daß der magnetische Gesamtfluß durch die Magnetogrammfläche verschwindet. Diese Methode wurde zur Berechnung des Magnetfeldvektors und der Feldlinien in der flare-aktiven Region vom August 1972 benutzt. Die berechneten Felder wurden mit anderen Beobachtungen, z. B. mit Hα-Strukturen, verglichen. Die Ergebnisse für den 3. August zeigen, daß das während der Flares vom 2. und 4. August beobachtete System von Bogenprotuberanzen durch ein kraftfreies Feld mit positivem α besser als durch ein stromfreies Feld ($\alpha = 0$) dargestellt werden kann. Der verfügbare Energieinhalt dieses kraftfreien Feldes ist von gleicher Größenordnung wie die für einen Flare maximal erforderliche Energie (10^{32} erg); die Höhenabhängigkeit der Magnetfeldstärke stimmt mit Schätzungen aus Radio- und Röntgen-Beobachtungen gut überein. Ähnliche Ergebnisse werden für die Magnetfeldstruktur am 7. August erhalten.

1. Introduction

Magnetic fields play a key role in almost all physical processes in solar active regions. Therefore there is a strong need for information about the magnetic field vector at all atmospheric levels. At present, however, reliable and detailed information about magnetic fields is available only for the photospheric level, where the inverse ZEEMAN effect in FRAUNHOFER lines is observable, most observations being restricted to the line-of-sight component only. The implications about magnetic fields that can be drawn from chromospheric and coronal observations, such as Hα fibrils and loops seen in EUV and X-ray lines, are very limited. Therefore, the measured line-of-sight component of the photospheric field must be extrapolated into the field vector in the higher layers. The most drastic simplification in doing this is to assume that the magnetic field is current-free (potential) above the photosphere. Surely, the main solar atmospheric magnetic field is caused by subphotospheric currents. However, the existence of electric currents in the chromosphere and in the corona is very likely. Many activity phenomena seem to be connected with magnetic field structures containing extractable energy and with changes in these configurations. For example, it is widely accepted that flares are caused by a release of stored magnetic energy. Since the subphotospheric currents are assumed not to be influenced by flares, atmospheric currents must exist as source of the flare energy.

Because of the dominance of the magnetic field and its stability in the chromosphere and lower corona, if appreciable currents are present, these must be aligned with the magnetic field, since otherwise the resulting LORENTZ forces could not be balanced by nonmagnetic forces (STURROCK and WOODBURY, 1967). Therefore, neglecting displacement currents,

$$\nabla \times \boldsymbol{B} = \alpha \boldsymbol{B} \,, \tag{1}$$

where α is, in general, a scalar function of position (and time). Due to difficulties in the mathematical treatment and in specifying the boundary conditions from observations, the practical application is confined to the case of α = constant. $\alpha = 0$ corresponds to the current-free case. Hitherto several methods were used to represent

© WILEY-VCH Verlag Berlin GmbH • Provided by the NASA Astrophysics Data System

1979AN....300..151S

current-free or constant α force-free magnetic fields above part or all of the solar surface (see LEVINE, 1975; SEEHAFER, 1978). They differ in the assumed boundary conditions which are used in addition to the measured photospheric magnetic field distribution (magnetogram).

The large active region of August 1972 presents a good opportunity to examine — by means of extrapolation — the role of magnetic fields in activity phenomena, since much observational material is available. Magnetic field extrapolation for this region has already been carried out by RUST and BAR (1973), using a current-free magnetic field representation, and by TANAKA and NAKAGAWA (1973), using a constant α force-free magnetic field representation and (instead of magnetograms) approximate photospheric line-of-sight data (single term FOURIER representation). The present study uses a new method to represent the constant α force-free magnetic field above a limited photospheric magnetogram area. Contrary to earlier extrapolation methods, this method does not require the net magnetic flux through the magnetogram area to be zero.

Some preliminary results of our extrapolation of the magnetic field of 1972 August 3 have already been published (SEEHAFER and STAUDE, 1977).

2. Magnetic Field Representation

In a system of Cartesian coordinates, x, y, z, let the domain of analysis be given by

$$0 \leqq x \leqq L_x\,, \qquad 0 \leqq y \leqq L_y\,, \qquad 0 \leqq z < \infty\,, \tag{2}$$

where $z = 0$ defines the plane of magnetograph observation. The magnetogram provides the boundary condition in terms of the vertical magnetic field component, B_z, at $z = 0$. To define a solution of (1), additionally boundary conditions on the vertical part of the boundary of the considered volume must be imposed. Let B_z vanish at the vertical planes $x = 0$, $x = L_x$, $y = 0$, $y = L_y$: it is assumed that the values of B_z at the boundary are small compared with its values at the inner parts of the cross section of the column. Then the components of the magnetic field are given in the forms (SEEHAFER, 1978)

$$B_x = \sum_{m,n=1}^{\infty} \frac{C_{mn}}{\lambda_{mn}} \mathrm{e}^{-r_{mn}z} \left\{ \alpha \frac{\pi n}{L_y} \sin\left(\frac{\pi m x}{L_x}\right) \cos\left(\frac{\pi n y}{L_y}\right) - r_{mn} \frac{\pi m}{L_x} \cos\left(\frac{\pi m x}{L_x}\right) \sin\frac{\pi n y}{L_y} \right\}, \tag{3a}$$

$$B_y = -\sum_{m,n=1}^{\infty} \frac{C_{mn}}{\lambda_{mn}} \mathrm{e}^{-r_{mn}z} \left\{ \alpha \frac{\pi m}{L_x} \cos\left(\frac{\pi m x}{L_x}\right) \sin\left(\frac{\pi n y}{L_y}\right) + r_{mn} \frac{\pi n}{L_y} \sin\left(\frac{\pi m x}{L_x}\right) \cos\left(\frac{\pi n y}{L_y}\right) \right\}, \tag{3b}$$

$$B_z = \sum_{m,n=1}^{\infty} C_{mn} \mathrm{e}^{-r_{mn}z} \sin\left(\frac{\pi m x}{L_x}\right) \sin\left(\frac{\pi n y}{L_y}\right), \tag{3c}$$

where the C_{mn} are defined by the expansion (3c) at $z = 0$,

$$\lambda_{mn} = \pi^2 \left(\frac{m^2}{L_x^2} + \frac{n^2}{L_y^2}\right). \tag{4}$$

and

$$r_{mn} = \sqrt{\lambda_{mn} - \alpha^2}\,. \tag{5}$$

The relation of the solution (3a, b, c) and the most relevant earlier solution, that of NAKAGAWA and RAADU (1972), is considered in detail by SEEHAFER (1978). For the practical application of the representation (3a, b, c), the magnetogram must be changed or completed in such a way that the values at the boundary vanish. In the present study an artificial zero boundary was added.

Due to the condition imposed on the vertical part of the boundary, the absolute value of α is limited. α^2 must be less than each of the numbers λ_{mn}, given by (4) ($m, n \geqq 1$), unless the corresponding Fourier coefficient C_{mn} vanishes. Therefore, in general, it must be

$$\alpha^2 < \alpha_{\max}^2 = \lambda_{11} = \pi^2 \left(\frac{1}{L_x^2} + \frac{1}{L_y^2}\right). \tag{6}$$

If C_{11} is zero or negligible in comparison with the other coefficients, as is the case for one of the used magnetograms, values of α^2 greater than λ_{11} are possible and α^2 is limited by the least of the remaining numbers λ_{mn}.

By means of Equations (3a, b, c) and an assumed value of α the magnetic field vector (B_x, B_y, B_z) may be calculated for each point (x, y, z) in the column above the magnetogram area (2). Moreover, the line of force through each such point may be computed in a given domain $z_1 \leqq z \leqq z_2$, and a plotter draws the lines of force in parallel projection in the demanded direction. A comparison of calculated lines of force with other chromospheric and coronal observations such as structures in H_α is necessary for selection of the optimum value of α. Practical calculations were carried out by means of a computer of type BESM-6. Values of (B_x, B_y, B_z) in a three-dimensional grid of points within the domain of analysis (2) are obtained very quickly, while the calculation of lines of force requires very much computer time. The computer programs have been tested for accuracy by means of well-known analytic solutions of (1) for α = constant. Inaccuracy caused by the discretness of the initial values $B_z(z = 0$ proved less than 15 percent.

© WILEY-VCH Verlag Berlin GmbH • Provided by the NASA Astrophysics Data System

1979AN....300..151S

Using Equations (3a, b, c), the magnetic energy contents of the considered active region may be calculated (in Gaussian units) according to

$$E_m = \frac{1}{8\pi}\int_V |B|^2\,\mathrm{d}V = \frac{L_x L_y}{32\pi}\sum_{m,n=1}^{\infty}\frac{C_{mn}^2}{r_{mn}}. \tag{7}$$

3. Observational Material

Many observations have been obtained all over the world from the big active region McMATH 11976 (Mt. Wilson 18935, USSR Solar Data No. 223/1972), therefore this complex sunspot group of August 1972 suggests itself for an investigation of the magnetic field structure by means of our method of extrapolation. We started our calculations from two digital Sacramento Peak magnetograms of August 3 and 7, the data of which are compiled in Table 1. The observations were obtained by means of the DOPPLER-ZEEMAN Analyzer which avoids saturation of the signal at large magnetic field strengths. Isogauss maps are given in the Figures 1 and 6.

Table 1. Magnetograms from the Sacramento Peak Observatory, 1972

Date	August 3	August 7
Time (h: min; UT)	23:20	16:30
Scan area (EW:NS)	610″:305″	399″:303″
Scan center	15°.5 N; 17°.6 E	17°.5 N;34°.8 W
Resolution (aperture; EW:NS)	6″.0:6″.0	7″.8:9″.5
Feet of calculated lines of force:		
a) whole region	30″:30″	30″:30″
b) central part (spot group)	6″:6″	

For comparison the following observed data have been used:
— two digital Kitt Peak magnetograms of August 2,
— magnetic maps from photographic observations at Potsdam on August 2 and 7 by means of a circular Zeeman analyzer,
— daily high resolution photospheric heliograms from Ondrejov during the period August 3 to 8,
— moreover many published data, among other observations those which have been compiled by the World Data Center A for Solarterrestrial Physics (COFFEY, 1973), in the papers by ZIRIN and TANAKA (1973), TANAKA and NAKAGAWA (1973), RUST and BAR (1973), and by the observers of IZMIRAN, Moscow (ISHKOV, 1976; KOROBOVA et al., 1976; LAZAREVA and MOGILEVSKY, 1976).

The observations show the following peculiar features of the magnetic field structure, which are of interest for an examination by means of extrapolation: The line of zero longitudinal magnetic field $B_{\|} \approx B_z(z = 0)$ in the photosphere shows a strong shear and high gradients, in its vicinity the penumbra filaments and Hα fibrils are arranged mainly parallel instead of perpendicular to the zero line, as it would have been expected for a potential field. A large dark filament in the NE of the active region was situated just above the zero line, outlining its twisted shape during the whole time of observations. Photographic Zeeman spectrograms show large amounts of ZEEMAN splitting near $B_{\|} = 0$, that is large transverse field components, indicating that the zero line is not a real neutral line at photospheric level.

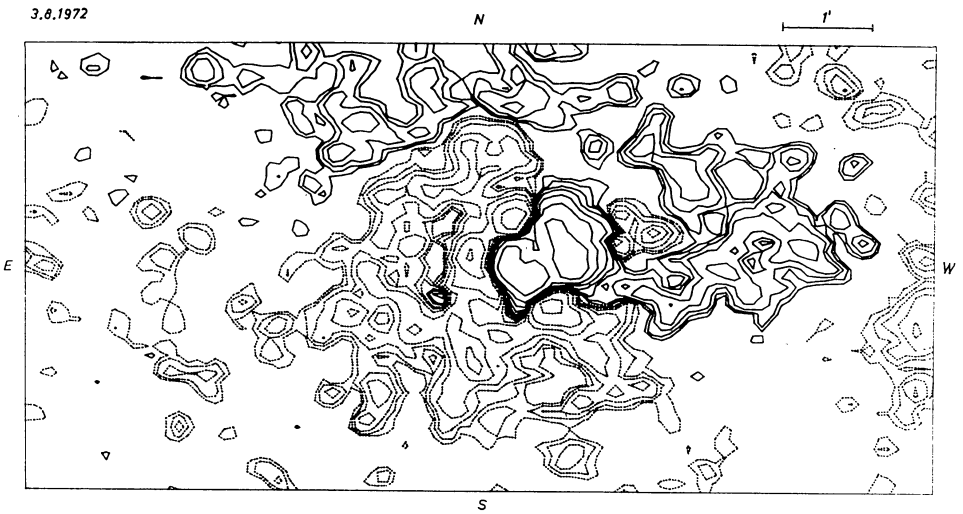

Fig. 1. Isogauss map of B_z for August 3. Solid contours are positive fields, dashed negative. Contour levels are 20, 40, 80, 160, 320, 640, and 1280 G.

© WILEY-VCH Verlag Berlin GmbH • Provided by the NASA Astrophysics Data System

1979AN....300..151S

During flares the loop prominence systems (LPS) or arch filament flare systems (AFFS) observed in H_α (BRUZEK, 1964) very probably outline the magnetic field structure in the higher levels up to some 100000 km above the photosphere. In our case the first loops formed at low chromospheric levels with orientations nearly parallel to the zero line, later the AFFS appeared increasingly higher with directions successively more perpendicular to the zero line. The higher loops run from the flare ribbon within the sunspot group to the east outside the group, that is mainly in EW direction. It is not yet clear if such a sequence of loops indicates a real change of the magnetic field from strongly sheared to nearly potential structures, or only a successive excitation of different loops of the field which remains unchanged during the flare but which is strongly sheared with height.

In spite of changes in the magnetic field fine structure in the photosphere and chromosphere from day to day the gross structure and topology remained practically unchanged, and it is very interesting to notice the almost identical structure and dynamics of the AFFS during the large flares of August 2, 4, 7, and 11, indicating the stability of the mean field structure. Similar conclusions have been drawn from observations of other flare-active regions, e.g. from XUV spectroheliograms from Skylab (CHENG, 1977).

4. Discussion of the Results and Conclusions

Examples of our extrapolations are given in the Figures 2 to 5 for August 3, and Figures 7 to 8 for August 7, information on details being given in the figure captions. More complete data are shown for the extrapolation of the August 3 magnetogram which has a better spatial resolution, a larger extent of the observed region, and a position closer to the center of the solar disk, as compared to the August 7 observations.

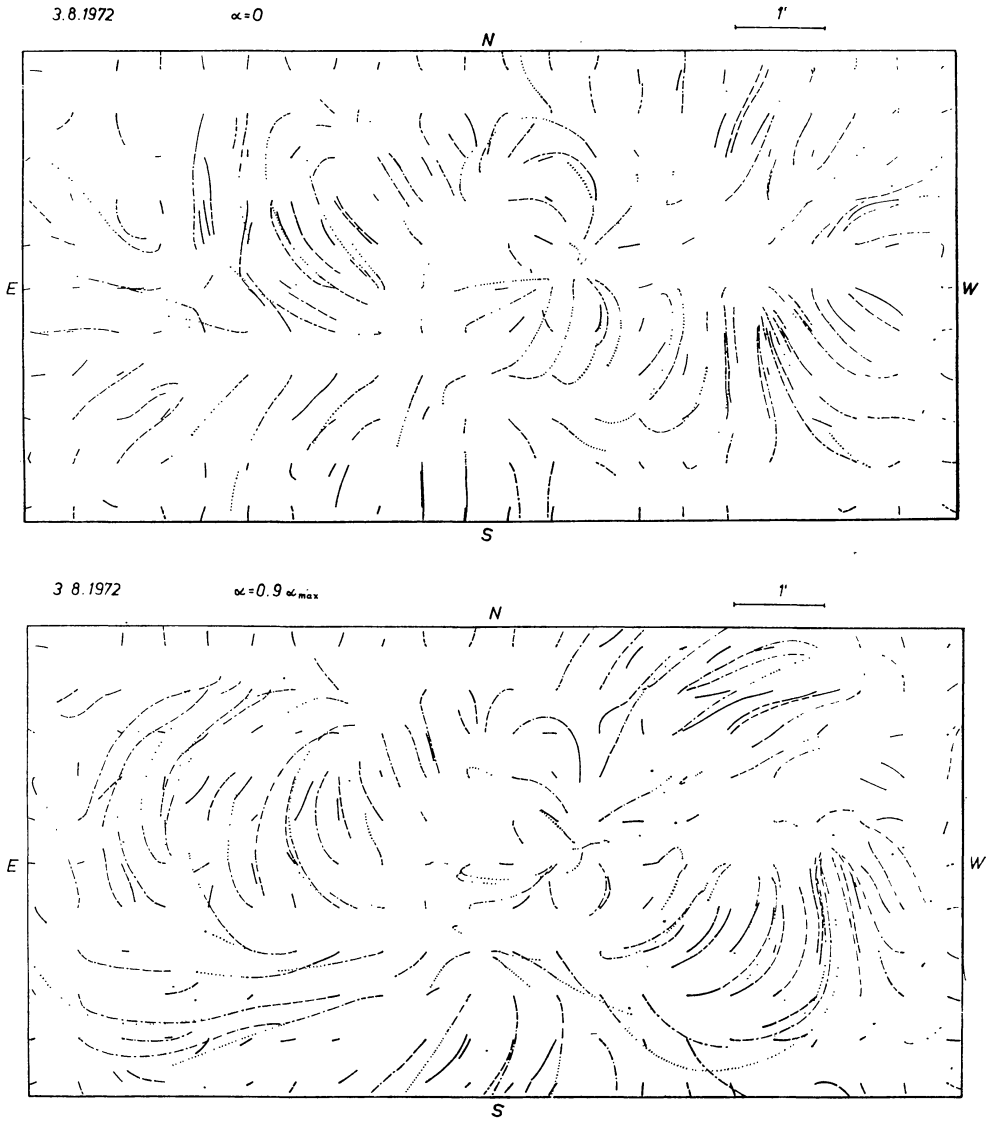

Fig. 2a, b. Lines of force calculated from the magnetogram of Fig. 1, starting from feet every 30″:30″, for two different values of α. The direction of projection is the same as during the observation (overview). Different heights above the photosphere are indicated by different contours: solid line 0—2000 km, dashed 2000—5000 km, dash-dot 5000—20000 km, dotted 20000—40000 km.

© WILEY-VCH Verlag Berlin GmbH • Provided by the NASA Astrophysics Data System

1979AN....300..151S

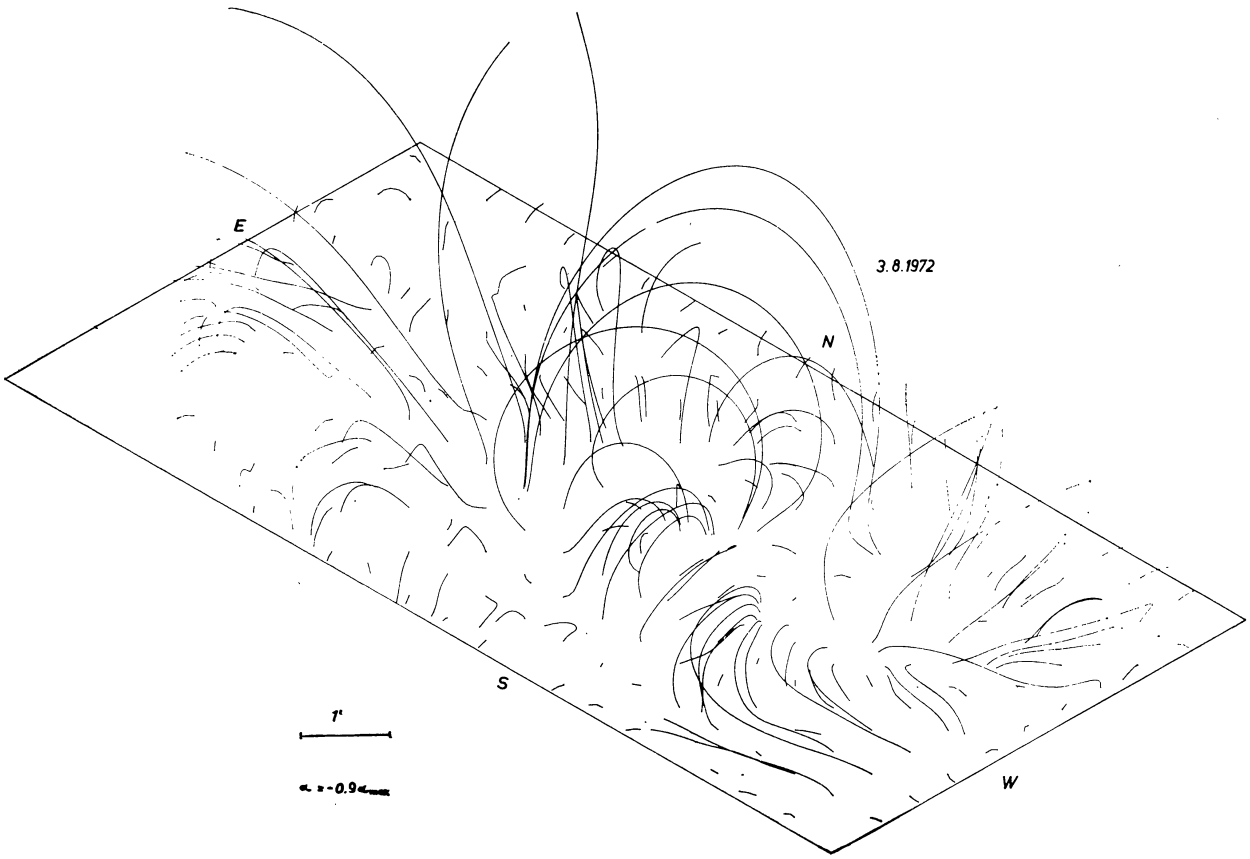

Fig. 3a

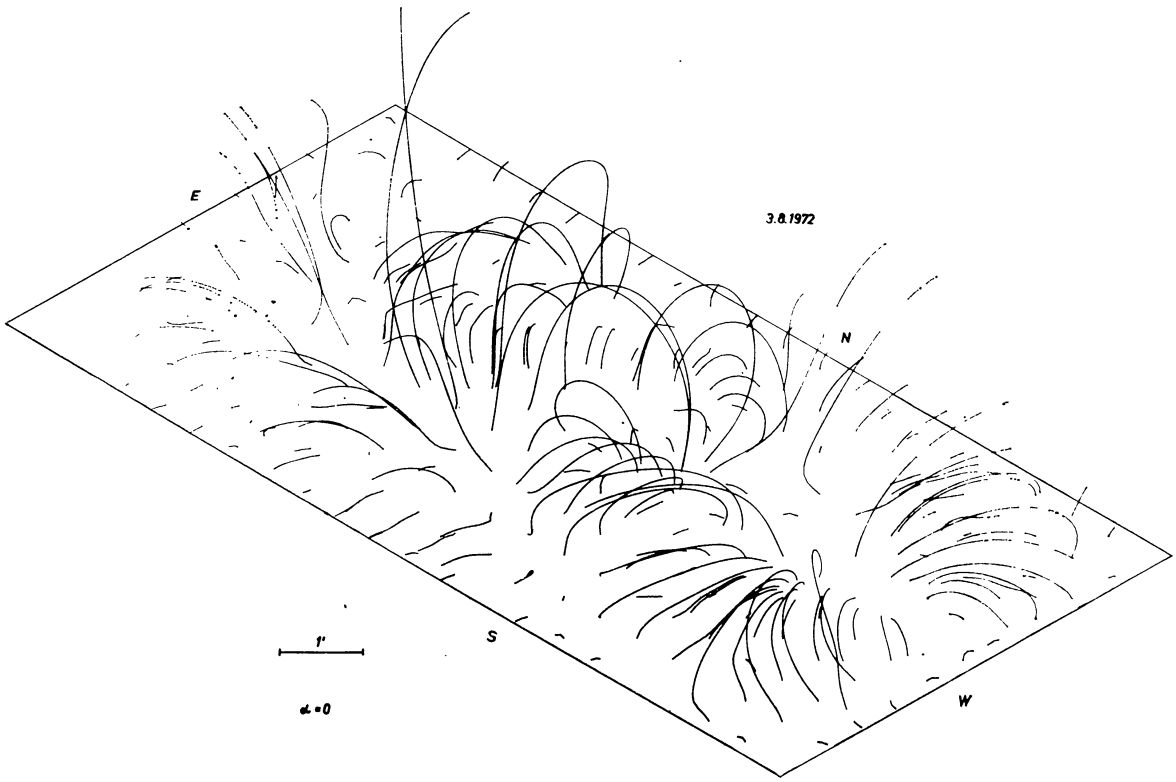

Fig. 3b

© WILEY-VCH Verlag Berlin GmbH • Provided by the NASA Astrophysics Data System

1979AN....300..151S

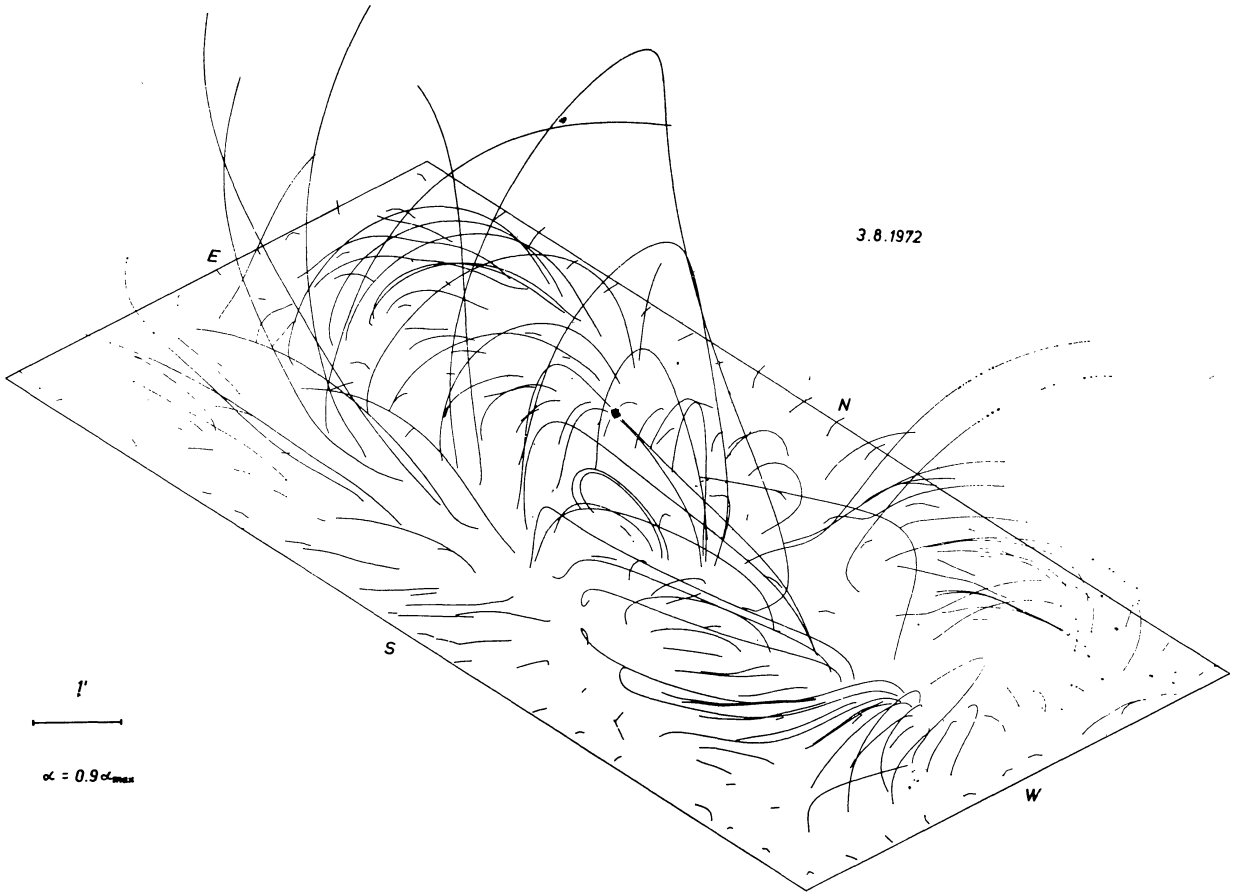

Fig. 3c

Fig. 3a, b, c. Lines of force for the same region as in the preceding figures, but now up to a height of 200000 km and drawn in isometric projection (perspective). Three different values of α are assumed.

Calculations of magnetic lines of force have been carried out for a potential magnetic field ($\alpha = 0$) as well as for large positive and negative values of $\alpha = \pm 0.9\,\alpha_{max}$, α being limited according to Equation (6). Because for the magnetogram of August 3 the first FOURIER coefficient C_{11} was small in comparison with the other coefficients, a calculation for a larger value of $\alpha = 0.9\,\alpha_{21}$ ($\alpha_{21}^2 = \lambda_{21}$) was possible. The lines of force are drawn in overview and perspective, starting from a mesh of feet every 30'':30'' in the photosphere for both days. For August 3 also a more dense mesh of 6'':6'' has been used for the central part (spot group) of the region, but information on the magnetic field structure of the whole magnetogram has been used when calculating the lines of force from this limited region. The calculated lines of force for August 3 are mainly compared with the AFFS observed during the flares of August 2 and 4, for August 7 with the AFFS observed at the same day. The results may be summarized as follows:

For $\alpha = 0$ we have obtained similar loops as RUST and BAR (1973), but only after omitting from our calculations other loops which do not fit as well with the observed AFFS. Indeed, the calculated lines of force for August 3 show a preferential direction from the spot group to the south rather than to the east as observed on August 2. For negative α the coincidence with observations is still worse, but for positive α most of the calculated loops in the considered region represent well the observed AFFS; similar results are obtained for August 7. Agreement between calculated lines of force and chromospheric Hα fibrils could not be obtained completely, but we thought it best for positive α too. The position of the large dark filament is discernible by arcades of supporting loops across the zero line in the NE. Projections of calculated lines of force against the west limb of the sun could be compared with observations of the AFFS on August 11, but well defined values of α are difficult to derive in this way. It is clearly to be seen, however, that the magnetic fields extend to larger heights with increasing absolute values of α.

Quantitative data on the three-dimensional magnetic field structure of an active region such as those obtained by our extrapolation are of great importance for calculations of models of active regions, for instance for models of X-ray and radio emissions from flares, and for estimates of the energy which may be stored in a special magnetic field configuration. Maximum values of the calculated magnetic field strength at different heights above the photosphere are given in Table 2. These values agree well with estimates from X-ray and radio observations, e.g., they are only 2 to 3 times larger than the average values of B above active regions compiled by DULK and MCLEAN (1978).

© WILEY-VCH Verlag Berlin GmbH • Provided by the NASA Astrophysics Data System

1979AN....300..151S

Equation (7) has been used to calculate the magnetic energy contents E_m in the considered active region for different α, results are given in Table 3. The energy supply of a force-free magnetic field extractable to be released during a flare may be estimated by subtracting E_m for $\alpha = 0$ from the E_m of the force-free field, because the potential field $\alpha = 0$ represents the field configuration with the minimum of E_m. It is interesting to note that the resulting values run to some 10^{32} ergs, that is to say they are of the order of magnitude of maximum flare demand.

The shortcomings of the method of extrapolation are for the most part due to incomplete observed data, that is usually only one component B_z at one level in a limited region is available, the data being still distorted

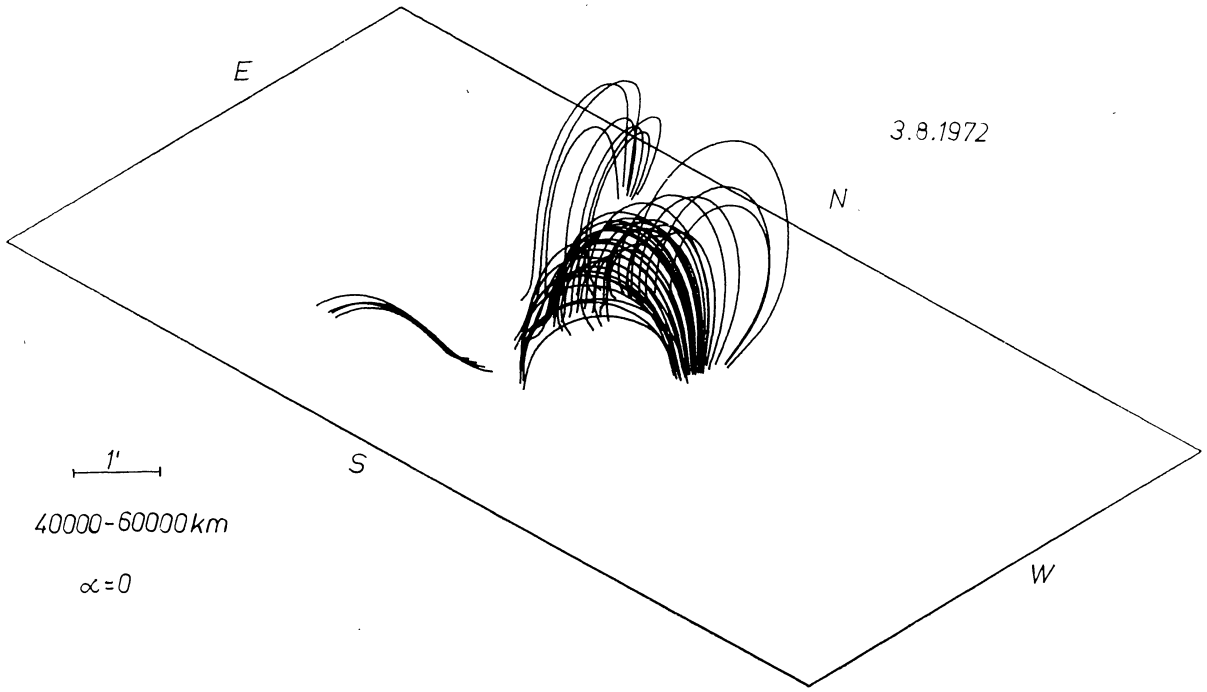

Fig. 4a

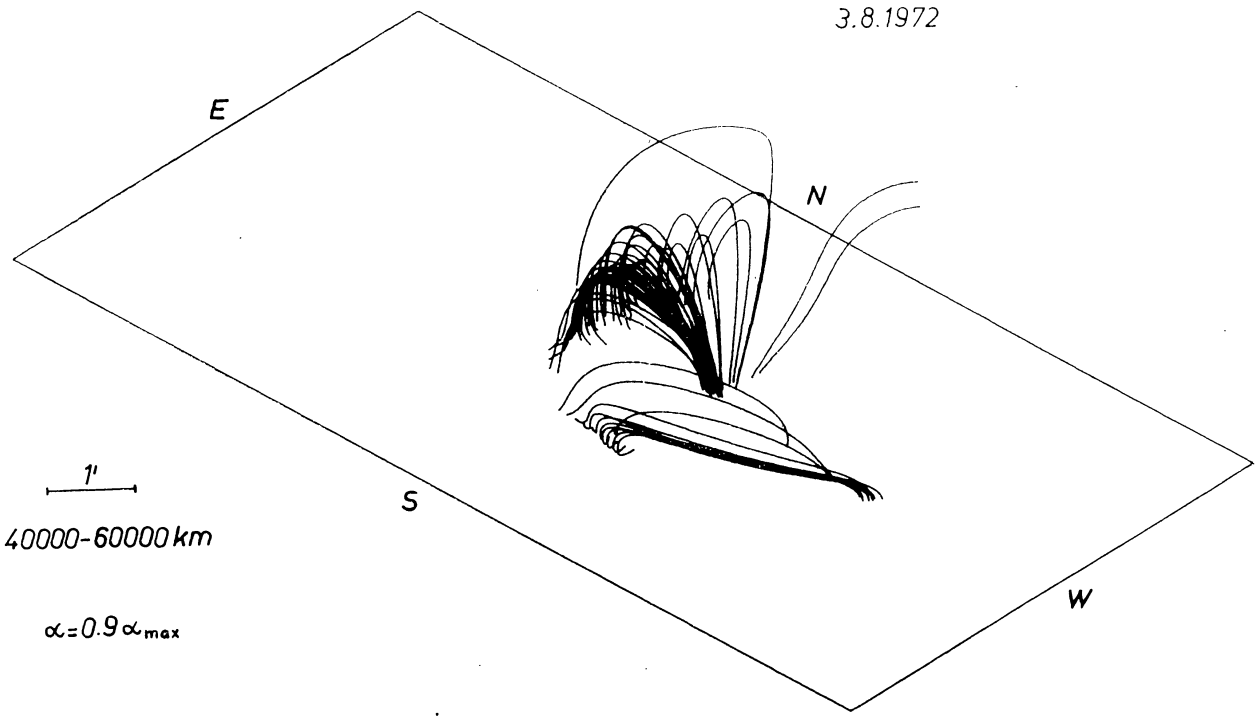

Fig. 4b

© WILEY-VCH Verlag Berlin GmbH • Provided by the NASA Astrophysics Data System

1979AN....300..151S

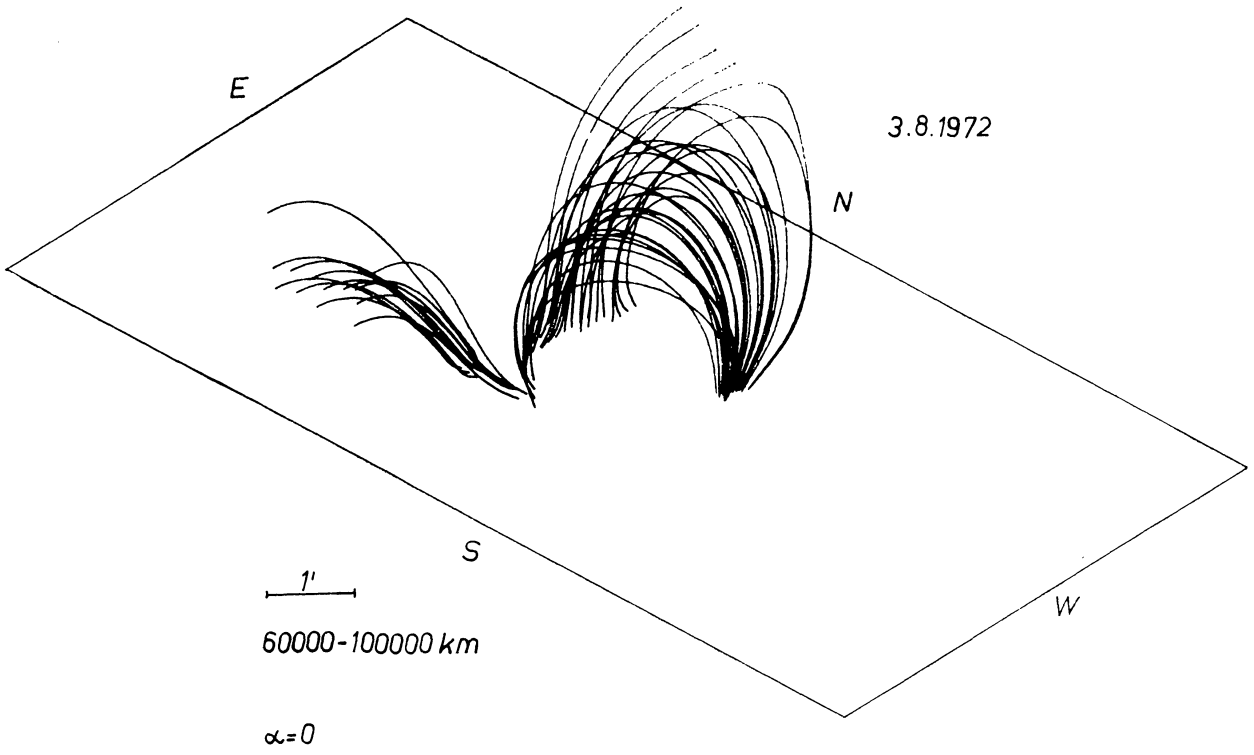

Fig. 4c

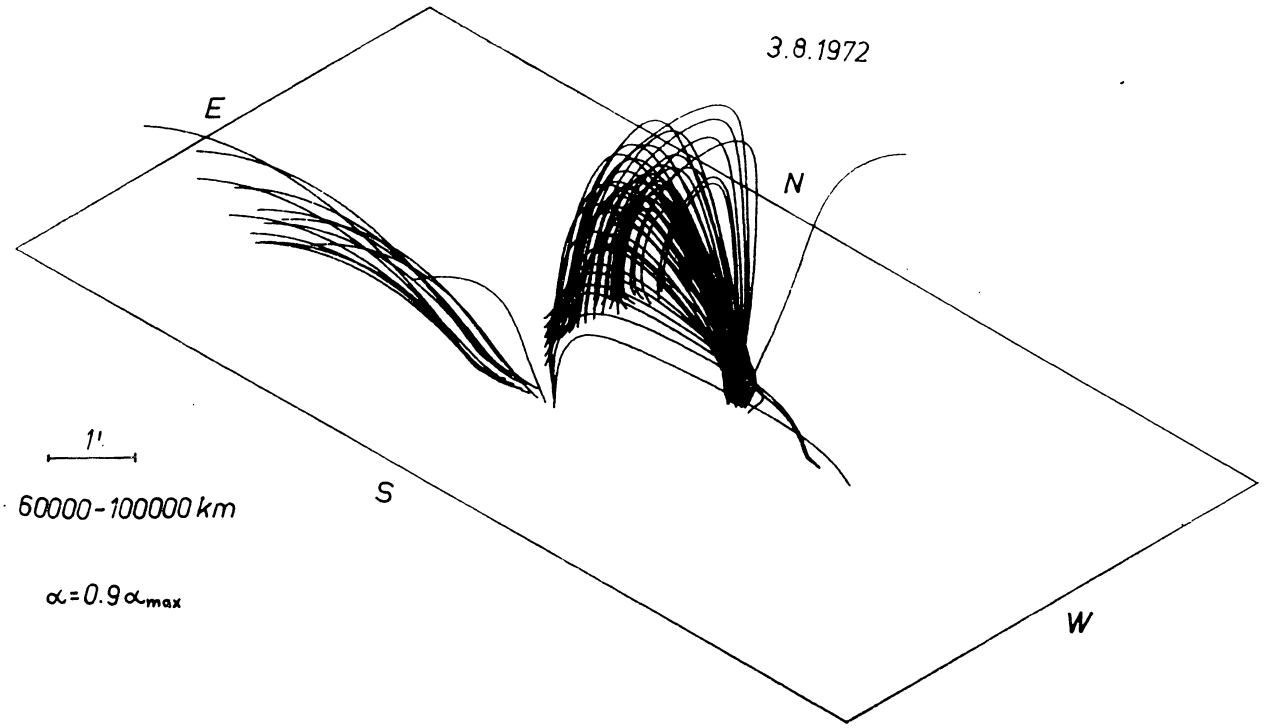

Fig. 4d

Fig. 4a, b, c, d. The same as Figures 3, but now the lines of force start from feet every·6″:6″ in the central part (spot group) of the active region, and only lines of force are drawn which turn back at domains of height 40000—60000 km and 60000—100000 km, respectively.

© WILEY-VCH Verlag Berlin GmbH • Provided by the NASA Astrophysics Data System

1979AN....300..151S

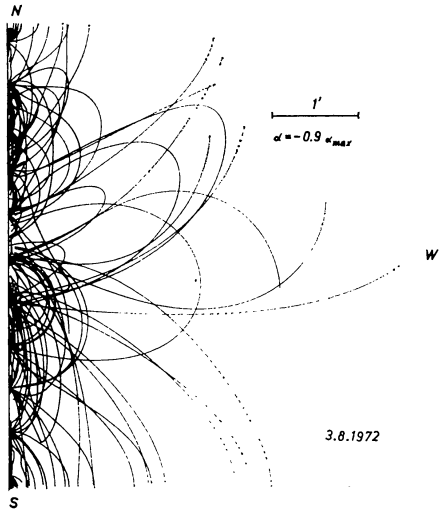

Fig. 5a

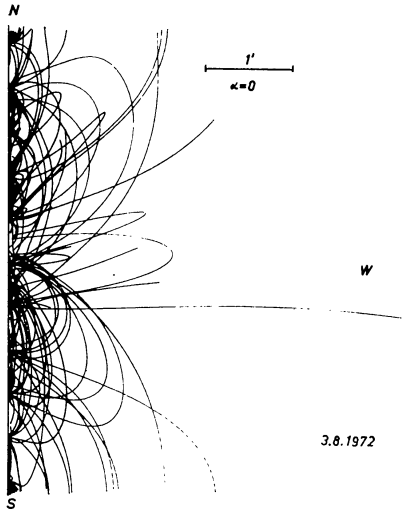

Fig. 5b

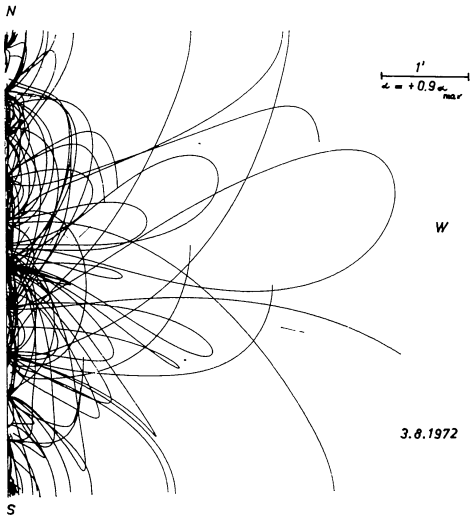

Fig. 5c

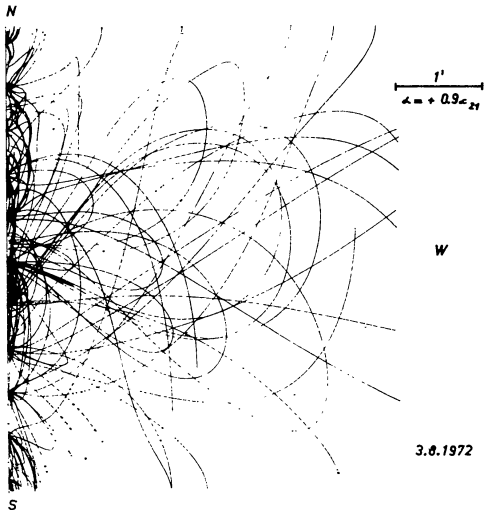

Fig. 5d

Fig. 5a, b, c, d. The same lines of force as in Figures 3, but now in a projection against the west limb of the sun. An additional very large value of $\alpha = 0.9\,\alpha_{21}$ has been assumed in 5d.

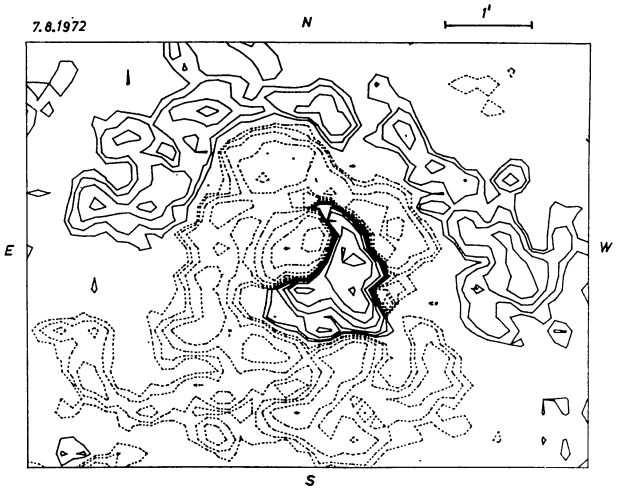

Fig. 6. The same as Figure 1, but now for August 7.

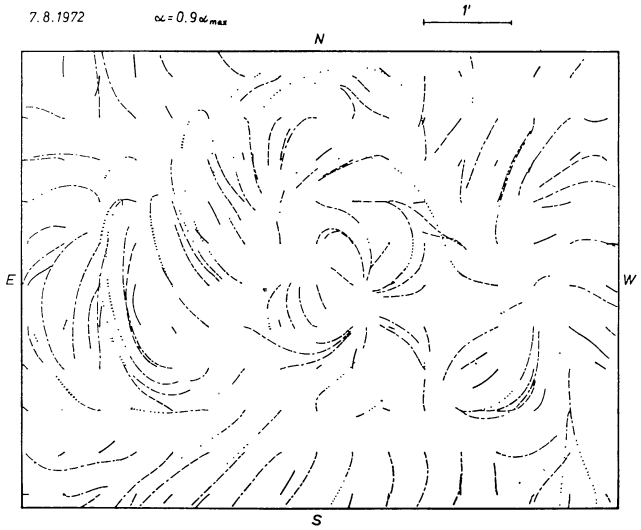

Fig. 7. The same as Figure 2b, but now for August 7.

© WILEY-VCH Verlag Berlin GmbH • Provided by the NASA Astrophysics Data System

1979AN....300..151S

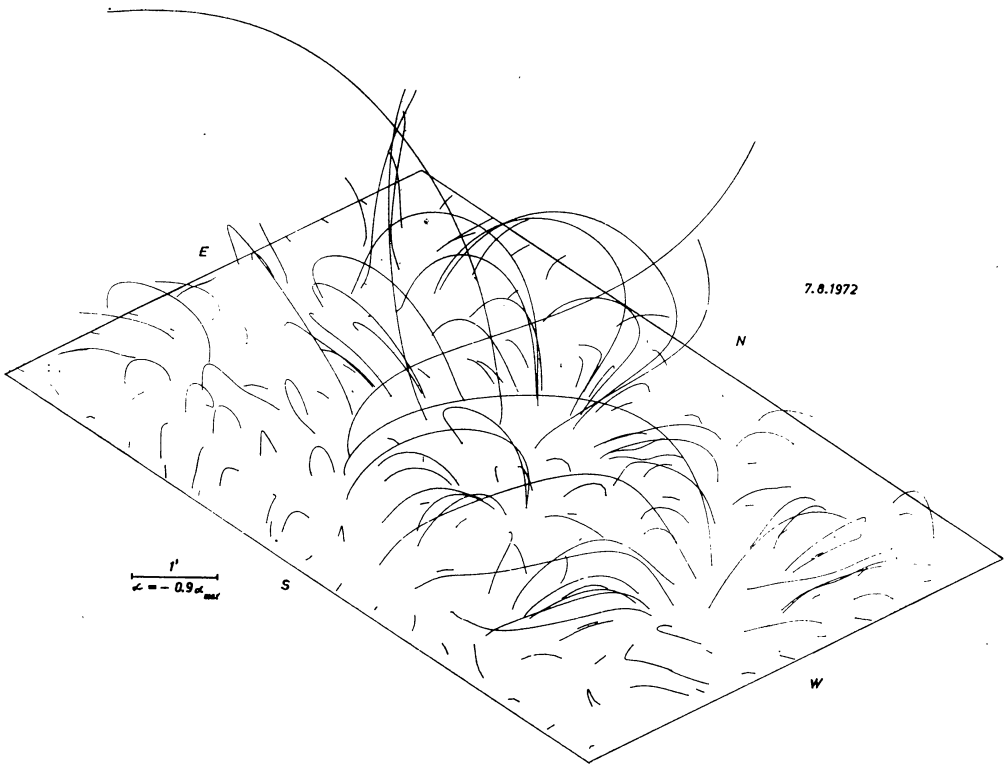

Fig. 8a

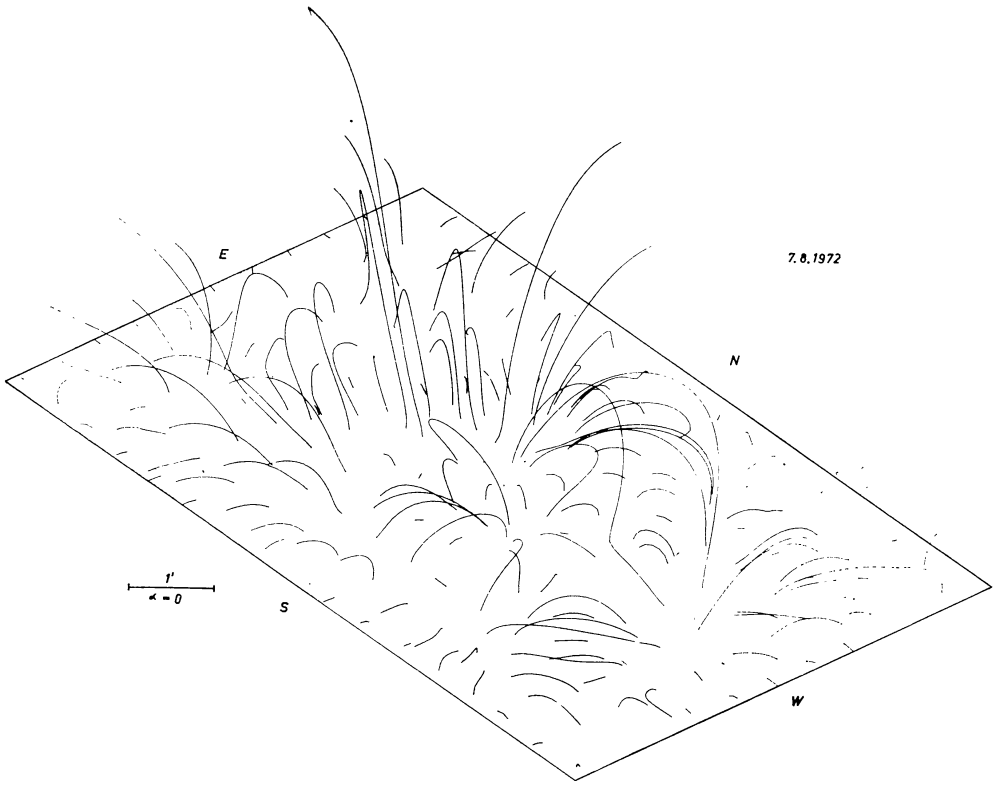

Fig. 8b

© WILEY-VCH Verlag Berlin GmbH • Provided by the NASA Astrophysics Data System

1979AN....300..151S

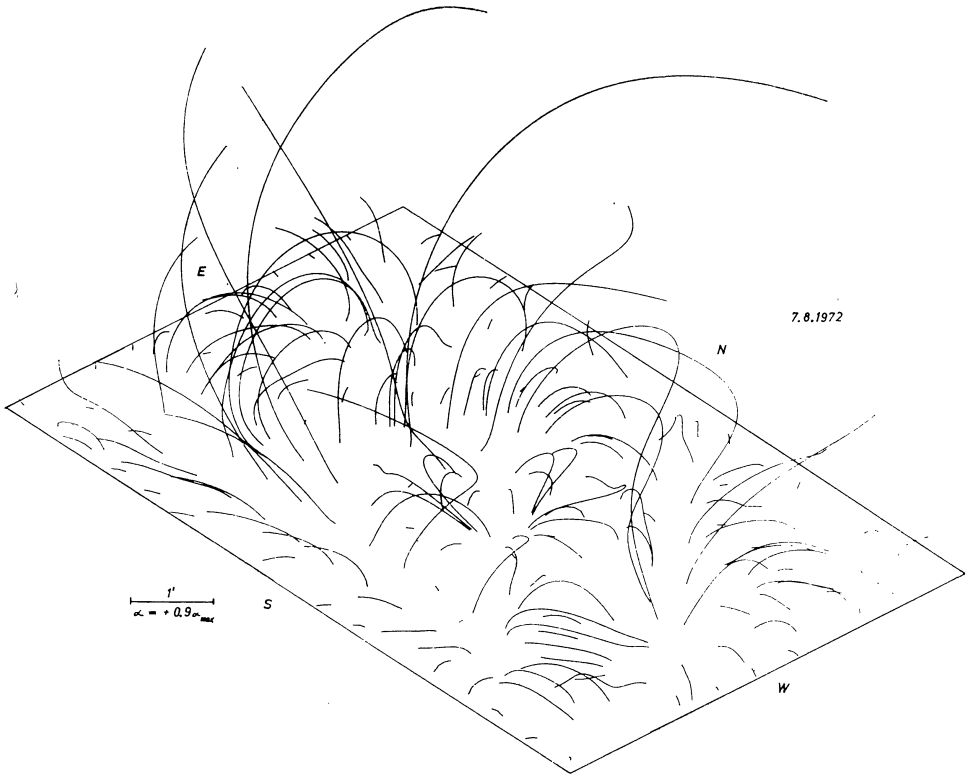

Fig. 8c

Fig. 8. The same as Figure 3a, b, c, but now for August 7.

Table 2. Maximum values of the magnetic field strength B_{max} (in G) at different heights z (in 10^6 m) above the photosphere, calculated for the August 3 magnetogram

z	B_{max} ($\alpha = 0$)	B_{max} ($\alpha = 0.9\alpha_{max}$)	B_{max} ($\alpha = -0.9\alpha_{max}$)
0	2263	2355	2192
4	1133	1068	1115
10	705	704	728
50	69	81	82
100	14	23	23

Table 3. Calculated magnetic energy content of the active region, August 3

α/α_{max}	0	0.5	0.9	0.99
E_m (in 10^{33} ergs)	2.28	2.32	2.44	2.50

by the moderate resolution power, instrumental polarization, and scattered light. Surely the assumption of $\alpha = $ const. in the whole region is an oversimplification, but models with variable α are impossible without additional observed data. Near the lateral boundary planes the disturbing influence of the unknown magnetic fields outside the considered region increases upward. By the present method the lateral boundary conditions are considered, however, in a more realistic way as compared with earlier attempts, because the net magnetic flux through the magnetogram area is not required to be zero and the lines of force are permitted to cross the lateral boundary planes in horizontal direction. Moreover, the reasonable results for the August 1972 active region (good representation of flare loops, height dependence of magnetic field strength, estimate of extractable energy supply) suggest that the mean magnetic field structure of the active region may be represented by a force-free field much better than by a potential field.

© WILEY-VCH Verlag Berlin GmbH • Provided by the NASA Astrophysics Data System

1979AN....300..151S

Acknowledgements

We are indebted to many colleagues who supplied their data for this study, in particular to Drs. D. M. RUST and R. Q. WADE from the Sacramento Peak Observatory for sending us magnetograms on punched cards, to Dr. W. C. LIVINGSTON for sending us listings of digital magnetograms from the Kitt Peak National Observatory, to Dr. J. SUDA for supplying high resolution heliograms from the observatory Ondrejov of the Czechoslovak Academy of Sciences, and to H. KÜNZEL for placing at our disposal ZEEMAN spectrograms from our observatory.

References

BRUZEK, A.: 1964, Astrophys. J. **140**, 746.
CHENG, C. C.: 1977, Solar Phys. **55**, 413.
COFFEY, H. E. (Ed.): 1973, World Data Center A for Solar-Terrestrial Physics, Report UAG-**28**, Part I.
DULK, G. A., and MCLEAN, D. J.: 1978, Solar Phys. **57**, 279.
ISHKOV, V. N.: 1976, in: Fizika solnechnoy aktivnosti (IZMIRAN), Nauka, Moskva, p. 45.
KOROBOVA, Z. B., ISHKOV, V. N., and MOGILEVSKY, E. I.: 1976, in: Fizika solnechnoy aktivnosti (IZMIRAN), Nauka, Moskva,, p. 3; Soln. dannye (USSR Solar Data) 10/1976, 92.
LAZAREVA, L. F., and MOGILEVSKY, E. I.: 1976, in: Fizika solnechnoy aktivnosti (IZMIRAN), Nauka, Moskva, p. 33; Soln. dannye (USSR Solar Data) 7/1976, 93.
LEVINE, R. H.: 1975, Solar Phys. **44**, 365.
NAKAGAWA, Y., and RAADU, M. A.: 1972, Solar Phys. **25**, 127.
RUST, D. M., and BAR, V.: 1973, Solar Phys. **33**, 445.
SEEHAFER, N.: 1978, Solar Phys. **58**, 215.
SEEHAFER, N., and STAUDE, J.: 1977, Proc. Intercosmos-KAPG-Seminar on Solar Physics in Debrecen 1977 (in press).
STURROCK, P. A., and WOODBURY, E. T.: 1967, in: Plasma Astrophysics, 39th E. Fermi School, Academic Press, New York and London, p. 155.
TANAKA, K., and NAKAGAWA, Y.: 1973, Solar Phys. **33**, 187.
ZIRIN, H., and TANAKA, K.: 1973, Solar Phys. **32**, 173.

Adress of the authors:

N. SEEHAFER, J. STAUDE
Zentralinstitut für solar-terrestrische Physik der Akademie der Wissenschaften der DDR
Sonnenabservatorium Einsteinturm
Telegrafenberg
DDR-15 Potsdam
German Democratic Republic

© WILEY-VCH Verlag Berlin GmbH • Provided by the NASA Astrophysics Data System